ISBN: 978-3-95450-262-2 ISSN: 2673-5350 doi: 10.18429/JACoW-IBIC2025-MOCC01

CURRENT ACTIVITIES OF BEAM DIAGNOSTICS IN THE J-PARC LINAC

K. Moriya†,[1], T. Miyao[2], M. Ishikawa[3], M. Chimura[1], H. Takahashi[1], Y. Morohashi[1], K. Takeishi[1], J. Kamiya[1]
[1]Japan Atomic Energy Agency (JAEA), 2-4 Shirakata, Tokai, Ibaraki, Japan
[2]KEK, 2-4 Shirakata, Tokai, Ibaraki, Japan
[3]Nuclear Engineering Ltd. (NECO), 2-4 Shirakata, Tokai, Ibaraki, Japan

Abstract

The J-PARC Linac accelerates a high-intensity beam of 50 mA using RF systems operating at 324 MHz and 972 MHz. To achieve stable acceleration and transport of such high-intensity beams, it is essential to measure the beam's current, centroid, and distribution in order to determine optimal operating conditions. This paper reports on the developments and improvements in linac beam diagnostics since 2015. As a specific example, carbon nanotubes have been implemented in the transverse profile monitor located at the upstream section of the linac, and no unintentional failures have occurred since this replacement. Additionally, this paper presents the current status and operational improvements of the longitudinal profile monitor.

INTRODUCTION

The Japan Proton Accelerator Research Complex (J-PARC) consists of three accelerators—the Linac, the 3 GeV Rapid Cycling Synchrotron (RCS), and the 50 GeV Main Ring Synchrotron (MR)—and three experimental facilities: the Materials and Life Science Experimental Facility (MLF), the Hadron Experimental Facility, and the Neutrino Experimental Facility [1].

The J-PARC Linac extracts negative hydrogen ions (H^-) generated from the ion source at 50 keV and accelerates them to 3 MeV using a Radio Frequency Quadrupole (RFQ) operating at 324 MHz. The beam is further accelerated to 50 MeV with a Drift Tube Linac (DTL), to 191 MeV with a Separated-type DTL (SDTL), and finally to 400 MeV with an Annular Coupled Structure (ACS) linac operating at 972 MHz. It is then injected into the RCS. In the RCS, the beam is accelerated to 3 GeV and subsequently transported to the MLF and the MR.

Figure 1 shows the time structure of the J-PARC Linac beam. To achieve a beam power of 1 MW in the RCS, the Linac delivers H^- beams accelerated to 400 MeV with a pulse width of 500 μs (macropulse) at a repetition rate of 25 Hz. Since the beam is accelerated at 324 MHz and 972 MHz, micropulses are formed at intervals of about 3 ns. In the RCS, which has a circumference of about 350 m, the beam is accelerated using RF at about 1 MHz. For matching with the RCS RF buckets, a portion of the beam is chopped in the Medium Energy Beam Transport 1 (MEBT1) between the RFQ and the DTL, producing an intermediate comb-like bunch structure. Thus, the time structures that must be monitored in the Linac are the microbunches for Linac beam matching and the intermediate bunches for matching to the RCS injection beam.

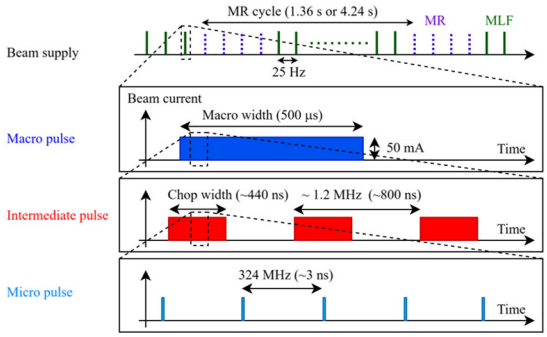

Figure 1: Time structure of J-PARC Linac's beam.

In general, to transport high-intensity beams without beam loss, it is necessary to measure the number of particles per bunch, the beam centroid positions in both transverse and longitudinal planes, and the transverse and longitudinal beam distributions. Here, the number of particles per bunch corresponds to the beam current, the beam centroid is expressed as (x, x', y, y', t, E), and the beam distribution as (α_x, β_x, ε_x, α_y, β_y, ε_y, α_z, β_z, ε_z). At the J-PARC Linac, beam tuning is performed using a commissioning software system consisting of JCE and XAL [2,3].

JCE is a development environment for creating beam tuning applications for the J-PARC Linac, based on the SAD scripting language developed at KEK. XAL is a beam dynamics and control software framework developed at the SNS in the U.S. [4]. It uses two configuration files: one describing the accelerator device parameters and another describing the beam properties, enabling beam simulations of the accelerator. The behavior of the beam centroid can be represented by a six-dimensional vector, while the behavior of the beam distribution can be reproduced using a 6×6 sigma matrix. In beam tuning, the optimal accelerator operating conditions are explored based on beam measurement results and beam simulations.

Table 1 summarizes the beam diagnostics employed for beam tuning and anomaly diagnosis in the J-PARC linac. Although several reports on the status of the J-PARC linac beam monitors have been published in the past, they date back more than eight years [5,6]. This paper provides an updated overview of the beam monitors, including recent developments and ongoing activities in the linac. Furthermore, it presents waveforms observed during abnormal

† moriya.katsuhiro@jaea.go.jp

ISBN: 978-3-95450-262-2 ISSN: 2673-5350 doi: 10.18429/JACoW-IBIC2025-MOCC01

Table 1: Monitor List

Monitor name	Measurement target	Direction
BLM	Beam loss	-
SCT	Beam current	-
FCT	Centroid position (Beam phase)	Long.
BSM	Profile	Long.
BPM	Centroid position	Trans.
WSM	Profile	Trans.

beam conditions encountered in beam tuning, together with their underlying causes.

BEAM LOSS MONITOR (BLM)

Figure 2 shows an external view of the Beam Loss Monitor (BLM) used to detect beam loss. At present, the J-PARC Linac employs a gas-filled proportional counter tube (E6876-600) manufactured by Canon Electron Tubes & Devices (formerly Toshiba Electron Tubes & Devices). When radiation enters the cylindrical tube filled with inert gas, the gas is ionized and electrons are generated. The electrons are accelerated by the high voltage applied between the cylindrical tube and the central wire, causing successive collisions and further ionization of the gas. Radiation is detected from the resulting electron signal. In total, 96 BLMs are installed throughout the J-PARC linac.

Figure 2: Beam Loss Monitor (Proportional counter tube).

During user operation, BLM signals are continuously monitored and recorded. If a signal exceeding a preset threshold is detected, the Machine Protection System (MPS) is triggered, and beam operation is temporarily suspended. The high voltage applied to the BLM is also monitored; if the specified voltage is not applied, the MPS is likewise triggered. The MPS modules and related components of the BLM are managed by the control group [7].

SLOW CURRENT TRANSFORMER (SCT)

Figure 3 shows the Slow Current Transformer (SCT) used to measure the beam current. The SCT employs a Finemet (FT-3M) core manufactured by Proterial (formerly Hitachi Metals) as a high-permeability magnetic material. The coil has 50 turns. The measurement accuracy of the SCT in the J-PARC Linac is better than ±0.1 mA. It should be noted that, as described later, the Fast Current Transformer (FCT) is also housed within the same case.

Until now, the SCT has been used to record the peak beam current. Recently, it was found that the peak current fluctuates at 2 MHz. This is because the ion source uses 2 MHz RF for plasma ignition, causing the extracted beam current to fluctuate. In addition, since the phase of this 2 MHz RF is not fixed, the SCT appeared to show shot-to-shot variations of a few percent in the peak current. Therefore, the waveform obtained from the SCT is now integrated over the entire macro pulse, and the result is recorded. This allows monitoring of all the bunches injected into the RCS, enabling accurate monitoring of the beam current transported to the experimental facilities.

At present, there are no major issues with the measurement performance of the beam monitors. However, the ceramic break has been damaged by the Great East Japan Earthquake and by earthquakes with a seismic intensity of 4 or higher [8]. At present, spare units are being prepared so that beam measurements can continue immediately even if a device fails.

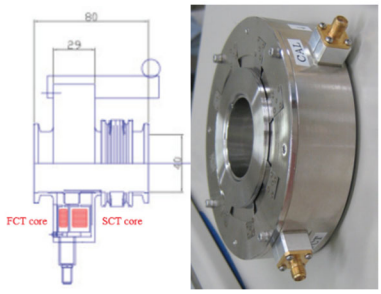

Figure 3: Layout of Current Transformer (SCT and FCT).

FAST CURRENT TRANSFORMER (FCT)

As described for the SCT, the Fast Current Transformer (FCT) is housed in the same case as the SCT (see Fig. 3). The core material is the same Finemet as used in the SCT, and the coil has a single turn. By using a phase detector to compare the FCT output with a reference signal (324 MHz) for monitoring, the phase difference is measured with a resolution of better than ±1 degree. In addition, two FCTs are used for energy measurements [9].

The FCT is primarily used for beam tuning and diagnosing abnormal beam conditions. During user operation, the FCT is rarely used, and adjustments are currently being made to enable its more effective utilization.

Figure 4 shows the Bunch Shape Monitor (BSM) used to measure the longitudinal beam distribution. The detailed operating principle is given in Feschenko's paper [10], and only a brief description is provided here. Using an actuator, a wire is inserted into the beam line. When the inserted wire interacts with the beam, it emits secondary electrons that inherit the same time structure as the beam. Owing to the –10 kV bias applied to the wire, the generated secondary electrons are accelerated to an energy of 10 keV. By applying the dipole field generated by the RF deflector, the longitudinal distribution of these electrons is converted into a transverse distribution, thereby enabling measurement of the longitudinal beam profile.

ISBN: 978-3-95450-262-2 ISSN: 2673-5350 doi: 10.18429/JACoW-IBIC2025-MOCC01

BUNCH SHAPE MONITOR (BSM)

At present, five BSMs are installed along the J-PARC beam line. Because each BSM was developed under different members at the time of installation, the component configurations have not been standardized. Although all BSMs are now capable of beam measurement, challenges remain before they can be fully utilized for beam tuning. Furthermore, due to the complexity of the system compared with other beam monitors, operation is currently limited to only a few members of the monitor group. To enhance its usability, we are working on establishing standardized measurement procedures and developing a graphical user interface (GUI). These efforts aim to build a new system in which not only the monitor group but also the beam tuning group can carry out beam measurements using the BSM. In this paper, we report on the chronological development and the current status of the J-PARC BSMs.

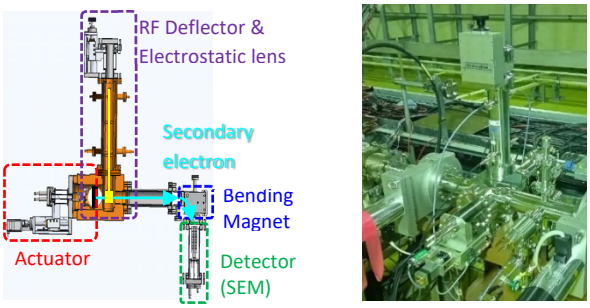

Figure 4: Layout of Bunch Shape Monitor.

INR-BSM (2012~2024)

To achieve longitudinal beam matching for transport from the SDTL to the ACS, J-PARC developed a BSM (INR-BSM) in collaboration with Feschenko and colleagues at the Institute for Nuclear Research (INR), Russian Academy of Sciences. Communication began around 2009, and three BSMs were fabricated and installed in 2012 at the planned ACS locations. Although successful measurements were obtained [11], it was later found during operation that the vacuum pressure increased up to 10^{-3} Pa, which interfered with the stable operation of the ACS cavities. The primary cause was insufficient surface treatment and cleaning of the vacuum chamber. To address this issue, one unit was relocated to MEBT2, between the SDTL and ACS, where it is currently in operation with three turbomolecular pumps (300 L/s for N_2) connected to increase pumping speed. Based on this experience, development of a successor model, the ACS-BSM, was initiated around 2014.

The INR-BSM was employed for measuring the longitudinal distribution, but it was not capable of deriving beam parameters such as Twiss parameters and emittance. Nevertheless, it proved effective for detecting longitudinal beam anomalies. For example, during beam tuning after long-term maintenance (50 mA, 50 μs), significant beam loss was observed at the first bending magnet in the L3BT. Since this was not due to quadrupole magnet mis-settings and could not be identified by the existing data acquisition system, a longitudinal anomaly at the head of the macrobunch was suspected, and measurements were performed using the INR-BSM. As shown in Fig. 5, the longitudinal distribution at the head of the macropulse was distorted, and the cause was traced to an inadequate feedforward setting in the LLRF. This figure represents the first achievement at J-PARC in detecting beam anomalies using the BSM.

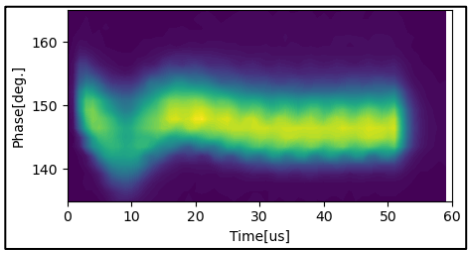

Figure 5: Beam anomaly measurement using INR:BSM.

In November 2024, one of the turbo-molecular pumps connected to this BSM suddenly stopped, leading to a degradation of the vacuum pressure. Although the exact cause remains unknown, it is presumed that the torque generated during the shutdown was transmitted to a nearby angle valve, resulting in deformation and vacuum leakage. As the development of the ACS-BSM is currently in progress, the malfunctioning INR-BSM has been removed from the beam line to avoid potential risks to accelerator operation.

ACS-BSM (Since 2015)

Three new BSMs (ACS-BSMs) were fabricated with improved surface treatment and cleaning of the vacuum chambers. In 2016, one ACS-BSM was installed near ACS1, and beam measurements were performed. The remaining two units were installed near ACS2 and ACS3 in 2018. However, no beam measurements were conducted between 2018 and 2023. The cause was found to be faulty connections, which prevented the proper application of high voltage to the electromagnetic amplifiers. Beam measurements resumed in 2024, and the ACS-BSMs are now being used as a replacement beam diagnostic system for the INR-BSM.

The ACS-BSMs are installed at locations adjacent to quadrupole magnets (QMs), both upstream and downstream. It was pointed out that secondary electrons might not reach the detector due to leakage fields from the QMs when transported from the beam line to the detector section, and magnetic shielding was therefore installed [12]. However, it was later found that the shielding was insufficiently fixed, causing it to move when the QMs were powered on or off. This prevented accurate estimation of the GL integral of the QMs, which would compromise proper beam tuning. Consequently, the magnetic shielding was removed in September 2023. It should be noted that beam transport to the downstream region is still achievable even with the upstream and downstream QMs turned off during ACS-BSM measurements, so secondary electrons can still be detected without the shielding.

ISBN: 978-3-95450-262-2 ISSN: 2673-5350 doi: 10.18429/JACoW-IBIC2025-MOCC01

Currently, the plan is to use three ACS-BSMs installed periodically to determine the beam parameters. However, if the measurement precision is insufficient, it may not be possible to accurately identify longitudinal mismatches, and thus verification of measurement accuracy is underway. This issue has also been recognized at the SNS in the United States [13].

MEBT1-BSM (Since 2015)

Around the same period as the development of the ACS-BSM, a BSM for MEBT1 (MEBT1-BSM) was developed to achieve longitudinal beam matching for transport from the RFQ to the DTL. Initially, a tungsten wire was employed, as with other devices. However, when exposed to the high-intensity beam, the wire frequently broke, preventing beam measurements. To address this, highly oriented pyrolytic graphite, which is more resistant to breakage, was adopted. With this material, beam measurements and calculations of beam parameters have now been successfully performed [14].

Nevertheless, the calculation of beam parameters currently requires more than 10 hours, making it infeasible to obtain results within the limited time available for beam tuning. In addition, although fixed magnetic shielding has been installed, the effect of the shielding on the magnetic field generated by the quadrupole magnets (QMs) has not yet been fully evaluated.

L3BT-BSM (Since 2018)

To observe the beam accelerated up to 400 MeV in the linac, a BSM (L3BT-BSM) was installed in the transport line between the linac and the RCS (L3BT). Based on experience with other BSMs, the longitudinal beam distribution can be measured; however, beam parameters have not yet been calculated. One issue is that an unused cavity located between the adjusted accelerating cavities and the L3BT-BSM accumulates an electric field when the beam passes through, which is shown in Fig. 6, which likely prevents accurate beam parameter determination. To address this, low-current tests and detuning of the cavity during measurements are being considered. This approach is expected to enable accurate beam parameter measurements.

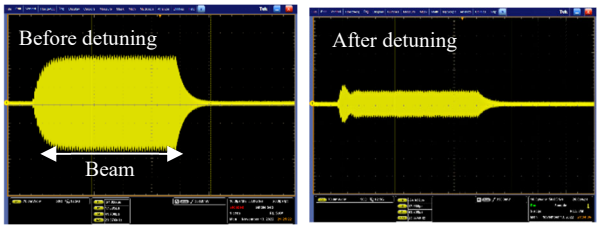

Figure 6: Unintended RF field in the acceleration cavity.

BEAM POSITION MONITOR (BPM)

Figure 7 shows the Beam Position Monitor (BPM), which adopts a stripline-type design, used to measure the horizontal and vertical beam centroids [15]. To ensure fast response and a wide dynamic range, the detection circuit employs the Log-Ratio method, achieving a dynamic range greater than 30 dB and a position resolution better than ±0.1 mm. This allows precise measurement not only of the 50 mA beam during user operation but also of low-current beams of approximately 5 mA during beam tuning. Due to installation constraints, all BPMs are mounted in conjunction with quadrupole magnets. Note that, due to space limitations, no BPMs are installed inside the Drift Tubes of the DTL. To date, no BPM has failed.

Recently, BPMs installed in the RCS injection line have been used to monitor and correct the energy of the injected beam [16]. BPMs placed at locations with finite dispersion detect energy deviations as position shifts. Based on these measurements, the phase of the last accelerating cavity in the linac is adjusted to correct the beam energy. By recording both the corrected energy and the predicted energy without correction, it was found that energy fluctuations were caused by variations in LLRF equipment due to humidity [17]. Currently, by placing some LLRF equipment in a temperature- and humidity-controlled chamber, the energy of the RCS injection beam has become highly stable.

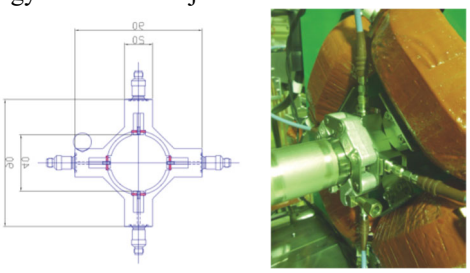

Figure 7: Layout of Beam Position Monitor.

WIRE SCANNER MONITOR (WSM)

Figure 8 shows the Wire Scanner Monitor (WSM) used to measure the horizontal and vertical beam profiles [18]. Two wires are mounted at right angles, each tilted 45° relative to the single-axis drive, allowing measurement of both projections. The drive employs a stepping motor (Oriental Motor Co., Ltd.) with 0.05 mm step resolution. Wire material depends on beam energy: carbon nanotube (CNT) wires, manufactured by Proterial, are used at MEBT1, while tungsten is used at higher energies. Since switching to CNT wires, no unintended breakage has occurred during beam measurements [19].

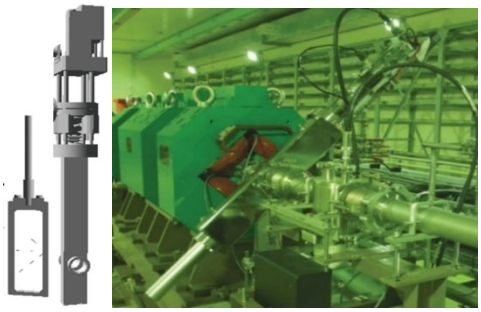

Figure 8: Layout of Wire Scanner Monitor.

The original motor driver was discontinued and replaced with a successor unit. Figure 9 compares beam profiles measured before and after the replacement. The vertical axis is normalized to the maximum signal. After the

ISBN: 978-3-95450-262-2 ISSN: 2673-5350 doi: 10.18429/JACoW-IBIC2025-MOCC01

update, the minimum detectable signal increased from 10^{-3} to ~10^{-2}, reducing the dynamic range by approximately one order of magnitude due to higher noise in the new driver. While sufficient for calculating the rms beam width required for tuning, this range is insufficient to detect beam abnormalities such as halo formation. Measures to reduce noise are currently under investigation.

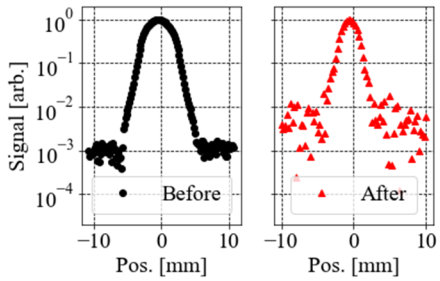

Figure 9: Transverse beam profile measurement using the WSM.

OTHER BEAM MONITORS

The SCT, BPM, and FCT are non-destructive monitors and can measure the beam during user operation, whereas the WSM and BSM are destructive and cannot. To address this, a Gas Sheet Monitor utilizing vacuum technology is being developed for non-destructive transverse beam measurements [20], and a laser-based system for both longitudinal and transverse profiling is also under development.

DATA ACQUISITION SYSTEM (DAQ)

The WE800 and WE900 (Yokogawa Electric), installed during construction, remain in operation, recording beam monitor waveforms roughly once per second rather than at 25 Hz. Similarly, the Wave Endless Recorder (Hitachi Zosen), introduced around the time of ACS installation, follows the same scheme. These systems present two limitations: they are no longer in production, and they monitor only the last intermediate pulse, preventing detection of anomalies at the start of a macro-pulse. To address this, a new data acquisition system capable of recording waveforms at 25 Hz, in addition to all intermediate pulses, is under development. In the RCS, such studies have already been conducted, while in the linac, µTCA.4-standard digitizers are being investigated.

CONCLUSION

At the J-PARC linac, beam monitors essential for the stable acceleration and transport of high-intensity beams are in continuous operation. Current efforts focus on upgrading the BSMs for longitudinal beam measurements and modernizing the data acquisition systems. In parallel, the replacement of Wire Scanner Monitor (WSM) drive units has led to increased noise, prompting an ongoing investigation into its cause. In addition, CNT wires have been successfully implemented in the WSM, preventing unintentional wire breakages observed in earlier designs. For non-destructive diagnostics, SCTs, BPMs, and FCTs enable beam monitoring during user operation, while new developments such as the Gas Sheet Monitor and laser-based diagnostics aim to measure both transverse and longitudinal beam profiles without interrupting beam delivery.

REFERENCES

[1] Y. Yamazaki ed., “The Joint Project for High-Intensity Proton Accelerators”, KEK Report 99-4, JAERI-Tech 99-056, 1999.

[2] H. Sako, C. K. Allen, H. Ikeda, and G. B. Shen, “Development of Commissioning Software System for J-PARC LINAC”, in *Proc. PAC'07*, Albuquerque, NM, USA, Jun. 2007, paper MOPAN044, pp. 257-259.

[3] H. Sako, *et al.*, “Unified Beam Control System of J-PARC Linac”, *IEEE Trans. Nucl. Science*, Vol. 57, No. 3, pp. 1528-1536, 2010.

[4] J. Galambos *et al.*, “XAL Application Programming Structure”, in *Proc. PAC'05*, Knoxville, TN, USA, May 2005, paper ROPA001, pp. 79-83.

[5] S. Lee *et al.*, “Upgrade of Beam Diagnostics in LEBT and MEBT of J-PARC LINAC”, in *Proc. LINAC'06*, Knoxville, TN, USA, Aug. 2006, paper TUP011, pp. 268-270.

[6] A. Miura *et al.*, "Design and Delivery of Beam Monitors for the Energy-upgraded Linac in J-PARC", *J. Korean Phys. Soc*. 66, 364, 2015.

[7] H. Takahashi *et al.,* “Update of MPS modules for J-PARC Linac and RCS”, *Proc. of PASJ2019*, 2019.

[8] A. Miura *et al.*, “Beam Monitor Deformation by Tohoku Earthquake and its Recovery Project”, in *Proc. IPAC'11*, San Sebastian, Spain, Sep. 2011, paper WEPC144, pp. 2328-2330.

[9] G. Shen and M. Ikegami, “Tuning of RF amplitude and phase for the separate-type drift tube linac in J-PARC”, *Nucl. Instrum. Methods Phys. Res. A* 598, 361, 2009.

[10] A. V. Feschenko, “Methods and Instrumentation for Bunch Shape Measurements”, in *Proc. PAC'01*, Chicago, IL, USA, Jun. 2001, paper ROAB002, pp. 517-521.

[11] A. Miura *et al.,* “Bunch Length Measurement of 181 MeV Beam in J-PARC Linac”, in *Proc. IPAC'13*, Shanghai, China, May 2013, paper MOPME027, pp. 532-534.

[12] J. Tamura *et a*l., “Numerical Study on the Effect of Magnetic Shield of a Bunch Shape Monitor in J-PARC Linac”, in *Proc. IPAC'13*, Shanghai, China, May 2013, paper THPWO035, pp. 3842-3844.

[13] A. Aleksandrov, "Operational Experience with BSMs at SNS", Topical Workshop on Bunch Shape Measurement, 2013.
kwwsv=22lqglfr1hvv1hx2hyhqw2772ryhuylhz

[14] R. Kitamura *et al.*, “Measurement of the longitudinal bunch-shape distribution for a high-intensity negative hydrogen ion beam in the low-energy region”, *Phys. Rev. Accel. Beams*, 26, 032802 , 2023.

[15] S. Lee *et al.,* “Systematic Calibration of Beam Position Monitor in the High Intensity Proton Accelerator (J-PARC) LINAC”, in *Proc. LINAC'04*, Lübeck, Germany, Aug. 2004, paper TUP70, pp. 429-431.

[16] K. Moriya *et al.*, "Energy measurement and correction for stable operation in J-PARC", *J. Phys.: Conf. Ser.* 1350 012140, 2019.

[17] K. Futatsukawa, private communication.

ISBN: 978-3-95450-262-2 ISSN: 2673-5350 doi: 10.18429/JACoW-IBIC2025-MOCC01

[18] S. Lee *et al.*, “Wire Profile Monitors in J-PARC Linac”, in *Proc. LINAC'06*, Knoxville, TN, USA, Aug. 2006, paper TUP021, pp. 293-295.

[19] A. Miura, K. Moriya, and T. Miyao, “Application of Carbon Nanotube Wire for Beam Profile Measurement of Negative Hydrogen Ion Beam”, in *Proc. IPAC'18*, Vancouver, Canada, Apr.-May 2018, pp. 5022-5025.
grl=4314;75<2MDFrZ0LSDF534;0IU[JEG6

[20] I. Yamada *et al.,* "High-intensity beam profile measurement using a gas sheet monitor by beam induced fluorescence detection", *Phys. Rev. Accel. Beams* 24, 042801, 2021.